Available online at www.sciencedirect.com

SciVerse ScienceDirect

Geochimica et Cosmochimica Acta 93 (2012) 205–213

Geochimica et Cosmochimica Acta

www.elsevier.com/locate/gca

# Isotope fractionation by diffusion in silicate melts: Insights from molecular dynamics simulations

Gaurav Goel [a,b], Liqun Zhang [a,b], Daniel J. Lacks [b], James A. Van Orman [a,b,*]

[a] Department of Earth, Environmental and Planetary Sciences, Case Western Reserve University, Cleveland, OH 44106, United States
[b] Department of Chemical Engineering, Case Western Reserve University, Cleveland, OH 44106, United States

Received 14 November 2011; accepted in revised form 9 July 2012; available online 20 July 2012

**Abstract**

Molecular dynamics simulations were performed to determine the isotope effect on diffusion in $SiO_2$ and $MgSiO_3$ liquids. The influence of an element's atomic mass on its diffusivity can be expressed in terms of the empirical relation $\frac{D_1}{D_2} = \left(\frac{m_2}{m_1}\right)^{\beta}$. For Si, $\beta$ has a value of ~0.05 in both $SiO_2$ and $MgSiO_3$ liquids, and is independent of pressure. The exponent $\beta$ for Mg in $MgSiO_3$ is larger, 0.135 at 1 atm, and decreases with pressure, to 0.084 at 50 GPa. Varying the mass and concentration of an isotope of one element is also found to have a significant influence on the diffusivity of other elements, due to the cooperative motions of the many atoms that are involved in diffusion. Interdiffusion between basaltic and rhyolitic magmas is inferred to be capable of producing isotope fractionations of tenths of per mil in Si, and tens of per mil in Mg. Significant diffusive fractionation of Si and Mg isotopes is also possible during the growth of olivine phenocrysts, if the growth rate is on the order of cm/yr or faster.


## 1. INTRODUCTION

Isotopes may be fractionated in magmatic systems both by equilibrium and kinetic processes. Equilibrium fractionation of isotopes between minerals and coexisting melt decreases rapidly with increasing temperature, and is generally quite small at magmatic temperatures. Kinetic separation of isotopes by diffusion through the melt, on the other hand, is not strongly temperature dependent and persists even at very high temperatures where equilibrium fractionation becomes negligible.

Diffusive separation of isotopes in the melt can be induced by a temperature gradient, as has been observed experimentally (Kyser et al., 1998; Richter et al., 2008, 2009; Huang et al., 2010) and hypothesized to occur in magma chamber zone-refining processes under certain conditions (Lundstrom, 2009). The physical mechanism for thermal isotope fractionation in silicate melts is not definitely established, but in general the behavior is consistent with results for simple hard sphere systems, where separation of isotopes results from elastic collisions and is due to the greater momentum of the heavier isotope, which always becomes enriched on the cold side of the temperature gradient (Lacks et al., 2012).

Isotope fractionation in magmas can also be induced by a gradient in chemical potential (Tsuchiyama et al., 1994; Richter et al., 1999, 2003; Watson and Müller, 2009). In this case the separation of isotopes is due to the mass dependence of their mobility: a heavier isotope diffuses more slowly, and will therefore lag behind a lighter isotope of the same element as both diffuse down the chemical potential gradient. Chemical potential gradients develop in a wide range of igneous processes – e.g. due to crystallization, recharge and mixing in magma chambers; partial melting and melt–rock reaction in the mantle; and chemical exchange between metal and silicates during core formation. Isotope fractionation by diffusion through the melt therefore may be important across a broad range of conditions, in cases where full chemical equilibrium is not achieved, if

* Corresponding author at: Department of Earth, Environmental and Planetary Sciences, Case Western Reserve University, Cleveland, OH 44106, United States.
*E-mail address:* james.vanorman@case.edu (J.A. Van Orman).

0016-7037/$ - see front matter © 2012 Elsevier Ltd. All rights reserved.
http://dx.doi.org/10.1016/j.gca.2012.07.008

the mass dependence of diffusivity is sufficiently large. Furthermore, it should be possible in many cases to use the observed fractionation of isotopes as a tool to determine the rates of these magmatic processes, provided that we know the difference in diffusivity of the isotopes at the conditions of interest.

The isotope effect on diffusion in silicate melts has been determined experimentally for only a few elements in a few compositional systems, at low pressures (Richter et al., 1999, 2003, 2008, 2009; Watkins et al., 2009, 2011). The dependence on mass is commonly expressed in the form:

$$\frac{D_1}{D_2} = \left(\frac{m_2}{m_1}\right)^{\beta} \quad (1)$$

where $D_1$ and $D_2$ are the diffusivities of two isotopes of the same element, with masses $m_1$ and $m_2$, and $\beta$ is an empirical scaling exponent (Richter et al., 1999; Watson and Baxter, 2007). The form of this equation is based on the kinetic theory of ideal gases, for which simple scaling relations show that molecular diffusion scales with molecular mass as described by Eq. (1), with $\beta = 0.5$. In silicate melts, diffusivity has been found to be both much less sensitive to the mass of the isotope than in an ideal gas and highly variable, with values of $\beta$ in the range ~0.02–0.2 for the small number of systems that have been investigated to date. In general, cations that diffuse rapidly relative to Si are found to have larger values of $\beta$ than those that diffuse slowly (Watkins et al., 2011). This relationship has been suggested to result from the degree of coupling between the cation and the silicate network; cations that are tightly bound to the network diffuse more slowly and with smaller mass selection because of their larger effective mass (Watkins et al., 2011).

Molecular dynamics (MD) simulations can provide important insight into atomic transport in liquids, and are especially well suited to the study of the isotope effect on diffusion. A particular advantage of MD simulations is that the mass and concentration of an isotope can be varied with all other parameters remaining precisely the same. This makes it possible to investigate how changing the mass and/or concentration of an isotope influences the diffusivities of other atoms in the system, due to their cooperative motions. In principle this could also be done in diffusion couple experiments, by changing the mix of isotopes used in different experiments, but in practice it is not possible to control the conditions or to determine the diffusion coefficients with enough precision to be able to resolve these small effects by comparing results from separate experiments.

Molecular dynamics simulations have been used to study the isotope effect on diffusion in simple monatomic (e.g. Kluge and Schober, 2000) and binary (Schober, 2001) Lennard–Jones liquids, liquid MgO (Tsuchiyama et al., 1994), and water (e.g. Bourg et al., 2010), but to our knowledge no previous study has been published on silicate liquids. The influence of pressure has been explored in monatomic Lennard–Jones liquids, where it has been found to reduce the mass dependence of diffusivity because diffusion in denser fluids is a more cooperative process that involves a greater number of atoms (Kluge and Schober, 2000). Silicate liquids are far more complicated than monatomic Lennard–Jones liquids because they have open polymerized structures that (1) collapse under increasing pressure, and (2) are modified by the addition of components such as MgO. These structural changes are known to have a strong influence on melt diffusivities and viscosity (e.g. Giordano and Dingwell, 2003; Lacks and Van Orman, 2007; de Koker et al., 2008; de Koker, 2010). To elucidate their influence on the isotope effect we performed simulations over a range of pressures, from 1 atm to 50 GPa, on both $SiO_2$ and $MgSiO_3$ liquids.

## 2. METHODS

The molecular dynamics simulations are carried out in an orthogonal simulation cell containing 2160 atoms, with periodic boundary conditions in all three dimensions. The simulations are run at constant-volume conditions corresponding to the volume at the pressure of interest; a preliminary constant-pressure simulation is used to determine the volume. The atomic interactions are based on the van Beest–Kramer–van Santen (BKS) potential for silica (van Beest et al., 1990), modified in two ways. First, a steep repulsive wall that is significant only at very short interatomic distances is added (Saika-Voivod et al., 2001), which is necessary because the short range repulsion in the BKS potential has a finite height that can be overcome in simulations at high temperatures. Second, the non-coulombic potential is truncated at 5.5 Å and shifted in energy such that the energy is continuous at this cutoff distance (Vollmayr et al., 1996), which leads to densities in better agreement with experiment. Coulombic interactions are summed by the Ewald method. The potential parameters are identical to those used by Lacks and Van Orman (2007) in simulations of a broad range of liquids in the $MgO–SiO_2$ system, which produce transport properties that are in good agreement with first-principles MD simulations (e.g. de Koker et al., 2008). The simulations were performed using several different codes — an in-house code, LAMMPS (Plimpton, 1995) and GROMACS (Hess et al., 2008). Consistent results were obtained in all cases.

To determine the diffusivities with sufficient precision to extract information on the isotope effect, the simulations must be carried out at high temperature and with an artificially large mass contrast between isotopes of the same element. All simulations are carried out at either 4000 or 4500 K, and the masses of the heavy isotopes are larger than those of the "normal" isotopes by a factor of 2–10. Similarly large mass differences have been used in MD simulations that address the isotope effect on diffusion of solutes in water, and the results are found to be in good agreement with experiment (Bourg et al., 2010).

In most of the simulations presented here, a fraction of the Si, Mg and/or O atoms are given a mass 2–10 times greater than their normal mass ($m_{Si} = 28$ g/mol, $m_{Mg} = 24$ g/mol, $m_O = 16$ g/mol). Control simulations, in which all atoms have normal masses, were also performed at most pressures and temperatures. The diffusivity for species $i$ is determined from the Einstein equation,

$$D_i = \frac{\langle \Delta r_i(t)^2 \rangle}{6t} \quad (2)$$

where $<\Delta r_i(t)^2>$ is the mean-squared displacement of atoms of type $i$ at time $t$. Most of the simulations were run for long times, up to 200 ns ($10^8$ time steps), to obtain precise estimates of the diffusion coefficients. Each simulation was divided into 20 equal time segments and the standard deviation of the mean value was taken as an estimate of the error. The diffusion coefficients determined in this study are self-diffusion coefficients. Each simulation considers a single homogeneous liquid composition (i.e. there are no chemical gradients in the simulation cell).

## 3. RESULTS AND DISCUSSION

Simulation results for liquid $SiO_2$ and $MgSiO_3$ are summarized in Tables 1 and 2, respectively. These tables include only data that were obtained from long simulations, of 100–200 ns duration, in which the diffusivities were determined with high precision.

The relationship between isotope diffusivity and isotope mass can be examined in terms of Eq. (1), where the mass sensitivity is given by $\beta = \ln(D_L/D_H)/\ln(m_H/m_L)$. We find no resolvable dependence of $\beta$ on temperature or on the proportion of heavy isotopes in the simulation cell, up to 28% (Fig. 1), and therefore consider together simulations with different isotope compositions, at 4000 and 4500 K, to determine the weighted mean value of $\beta$ for each element at each pressure. These weighted mean values are summarized in Table 3. For Si in $SiO_2$, $\beta = 0.055 \pm 0.005$ at atmospheric pressure. This value is in reasonable agreement with the analogous experimental determination for diffusion of Ge isotopes in $GeO_2$, where $\beta$ is constrained to be less than ~0.05 (Richter et al., 1999). The mass dependence of Si isotope diffusion does not appear to be sensitive to melt composition, as the $\beta$ values in $MgSiO_3$ are within error of the value in $SiO_2$. Also, $\beta_{Si}$ does not vary significantly with pressure in either $SiO_2$ or $MgSiO_3$ (Fig. 2), despite substantial changes in density, melt structure and transport properties over the pressure range we studied (Lacks and Van Orman, 2007).

The mass dependence of Mg diffusion is significantly larger than for Si, with $\beta_{Mg} = 0.135 \pm 0.008$ in $MgSiO_3$ at atmospheric pressure. This value is somewhat higher than the value $\beta_{Mg} = 0.05$ found by Richter et al. (2008) in chemical diffusion experiments using basalt–rhyolite diffusion couples, but similar to the value $\beta_{Mg} = 0.1$ found by Watkins et al. (2011) in chemical diffusion experiments using albite–diopside couples. The mass dependence we find for Mg self-diffusion at 1 atm also is not very different from the value $\beta_{Ca} \sim 0.05$–0.1 found for Ca in self-diffusion experiments with $CaO$–$Al_2O_3$–$SiO_2$ melts (Richter et al., 1999). In contrast to Si, the mass dependence of Mg self-diffusion in our simulations decreases significantly with pressure, becoming closer to the value for Si as pressure increases (Fig. 2).

In simple monatomic Lennard–Jones liquids, the mass dependence of isotope diffusion has been found to decrease with increasing pressure (Kluge and Schober, 2000). This behavior was explained in terms of the greater cooperativity of the motions involved in diffusion at high pressures – the denser the liquid, the larger the number of neighboring atoms are needed to move cooperatively to allow a diffusive jump. Silicate liquids are different from simple Lennard–Jones liquids in that they have open, but relatively strong, silicate network structures at low pressures. At higher pressures the network structure gradually collapses and the liquid adopts a denser, more close-packed structure (Lacks and Van Orman, 2007; de Koker et al., 2008; de Koker, 2010). These structural changes occur gradually over

Table 1
$SiO_2$ liquid results. All simulations were performed with 2 fs step interval and $5 \times 10^7$ to $1 \times 10^8$ timesteps, with all oxygen atoms having normal mass (16 amu).

| $T$ (K) | $P$ (GPa) | $m_{Si,H}/m_{Si,N}$ | $x_{Si,H}$ | $D_{Si,N}$ ($10^{-9}$ m$^2$/s) | $D_{Si,H}$ ($10^{-9}$ m$^2$/s) | $D_O$ ($10^{-9}$ m$^2$/s) |
|---|---|---|---|---|---|---|
| 4500 | 0 | – | 0 | 1.545 ± 0.007 | – | 2.104 ± 0.010 |
| 4500 | 0 | 2 | 0.014 | 1.545 ± 0.007 | 1.523 ± 0.041 | 2.104 ± 0.010 |
| 4500 | 0 | 2 | 0.069 | 1.528 ± 0.010 | 1.477 ± 0.024 | 2.086 ± 0.005 |
| 4500 | 0 | 2 | 0.28 | 1.491 ± 0.014 | 1.448 ± 0.014 | 2.038 ± 0.007 |
| 4500 | 0 | 4 | 0.014 | 1.535 ± 0.006 | 1.430 ± 0.041 | 2.098 ± 0.009 |
| 4500 | 0 | 4 | 0.069 | 1.516 ± 0.009 | 1.418 ± 0.036 | 2.071 ± 0.007 |
| 4500 | 0 | 4 | 0.28 | 1.440 ± 0.006 | 1.337 ± 0.012 | 1.949 ± 0.009 |
| 4500 | 0 | 10 | 0.014 | 1.536 ± 0.008 | 1.334 ± 0.035 | 2.092 ± 0.005 |
| 4500 | 0 | 10 | 0.069 | 1.496 ± 0.006 | 1.318 ± 0.015 | 2.032 ± 0.005 |
| 4500 | 0 | 10 | 0.28 | 1.340 ± 0.005 | 1.174 ± 0.011 | 1.799 ± 0.005 |
| 4000 | 0 | – | 0 | 0.372 ± 0.006 | – | 0.537 ± 0.007 |
| 4000 | 0 | 4 | 0.069 | 0.365 ± 0.005 | 0.338 ± 0.007 | 0.531 ± 0.003 |
| 4000 | 0 | 4 | 0.28 | 0.343 ± 0.003 | 0.319 ± 0.005 | 0.496 ± 0.004 |
| 4500 | 10 | – | 0 | 4.626 ± 0.053 | – | 5.977 ± 0.044 |
| 4500 | 10 | 4 | 0.28 | 4.324 ± 0.024 | 4.029 ± 0.030 | 5.531 ± 0.021 |
| 4000 | 20 | – | 0 | 3.181 ± 0.053 | – | 4.035 ± 0.078 |
| 4000 | 20 | 4 | 0.069 | 3.101 ± 0.037 | 2.882 ± 0.077 | 3.964 ± 0.021 |
| 4000 | 20 | 4 | 0.28 | 2.952 ± 0.022 | 2.740 ± 0.034 | 3.720 ± 0.017 |
| 4500 | 40 | – | 0 | 3.909 ± 0.024 | – | 4.730 ± 0.035 |
| 4500 | 40 | 4 | 0.28 | 3.618 ± 0.015 | 3.400 ± 0.018 | 4.367 ± 0.012 |

Table 2
$MgSiO_3$ liquid results. All simulations were performed at 4000 K with 2 fs step interval and $5 \times 10^7$ to $1 \times 10^8$ timesteps, with all oxygen atoms having normal mass (16 amu).

| $P$ (GPa) | $m_{Si,H}/m_{Si,N}$ | $m_{Mg,H}/m_{Mg,N}$ | $x_H$ | $D_{Si,N}$ ($10^{-9}$ m$^2$/s) | $D_{Si,H}$ ($10^{-9}$ m$^2$/s) | $D_{Mg,N}$ ($10^{-9}$ m$^2$/s) | $D_{Mg,H}$ ($10^{-9}$ m$^2$/s) | $D_O$ ($10^{-9}$ m$^2$/s) |
|---|---|---|---|---|---|---|---|---|
| 0 | – | – | 0 | $5.945 \pm 0.029$ | – | $25.50 \pm 0.17$ | – | $8.051 \pm 0.009$ |
| 0 | 1 | 4 | 0.116 | $5.871 \pm 0.043$ | – | $24.951 \pm 0.081$ | $20.676 \pm 0.222$ | $7.897 \pm 0.011$ |
| 0 | 1 | 4 | 0.231 | $5.702 \pm 0.024$ | – | $24.397 \pm 0.104$ | $20.219 \pm 0.152$ | $7.735 \pm 0.010$ |
| 0 | 4 | 1 | 0.116 | $5.866 \pm 0.041$ | $5.452 \pm 0.081$ | $25.293 \pm 0.146$ | – | $7.881 \pm 0.020$ |
| 0 | 4 | 4 | 0.116 | $5.730 \pm 0.017$ | $5.393 \pm 0.066$ | $24.837 \pm 0.094$ | $20.642 \pm 0.216$ | $7.737 \pm 0.039$ |
| 25 | – | – | 0 | $4.072 \pm 0.026$ | – | $9.6 \pm 0.056$ | – | $5.653 \pm 0.009$ |
| 25 | 1 | 4 | 0.116 | $4.003 \pm 0.015$ | – | $9.372 \pm 0.027$ | $8.040 \pm 0.09$ | $5.581 \pm 0.015$ |
| 25 | 1 | 4 | 0.231 | $3.943 \pm 0.024$ | – | $9.011 \pm 0.072$ | $8.106 \pm 0.027$ | $5.483 \pm 0.019$ |
| 25 | 1 | 4 | 0.5 | $3.752 \pm 0.014$ | – | $8.630 \pm 0.067$ | $7.653 \pm 0.039$ | $5.284 \pm 0.013$ |
| 25 | 4 | 1 | 0.116 | $3.984 \pm 0.026$ | $3.640 \pm 0.069$ | $9.422 \pm 0.074$ | – | $5.560 \pm 0.020$ |
| 25 | 4 | 4 | 0.116 | $3.948 \pm 0.018$ | $3.732 \pm 0.016$ | $9.245 \pm 0.044$ | $8.076 \pm 0.083$ | $5.439 \pm 0.017$ |
| 25 | 4 | 4 | 0.25 | $3.762 \pm 0.012$ | $3.551 \pm 0.040$ | $8.700 \pm 0.057$ | $7.667 \pm 0.044$ | $5.238 \pm 0.015$ |
| 50 | – | – | 0 | $2.240 \pm 0.014$ | – | $5.10 \pm 0.03$ | – | $2.985 \pm 0.009$ |
| 50 | 4 | 4 | 0.116 | $2.140 \pm 0.018$ | $2.0005 \pm 0.033$ | $4.909 \pm 0.035$ | $4.371 \pm 0.040$ | $2.880 \pm 0.009$ |

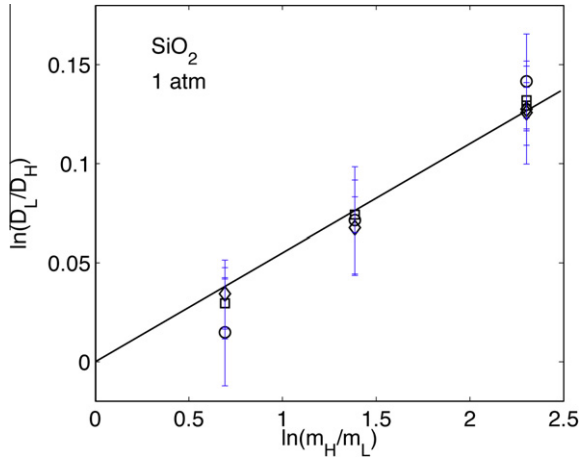


Fig. 1. Diffusivity of silicon isotopes in liquid $SiO_2$ as a function of the mass of the isotope, at 1 atm and 4500 K. The circles represent simulations in which heavy Si atoms comprise 1.4% of the Si atoms in the system, diamonds represent 6.9% heavy Si and squares represent 28% heavy Si. Note that the diffusivity results from simulations with fewer heavy atoms have larger errors. The data are consistent with $\beta = 0.055 \pm 0.005$.

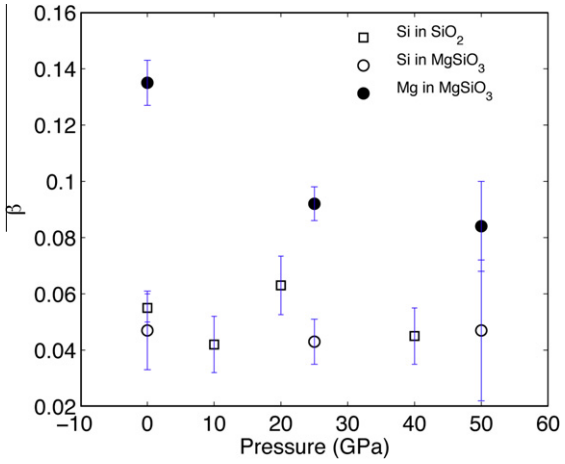


Fig. 2. Variation in $\beta$ with pressure, for Si and Mg in liquid $SiO_2$ and $MgSiO_3$.

Table 3
Summary of results for $\beta$ in $SiO_2$ and $MgSiO_3$.

| Composition | Element | $P$ (GPa) | $\beta$ |
|---|---|---|---|
| $SiO_2$ | Si | 0 | $0.055 \pm 0.005$ |
| $SiO_2$ | Si | 10 | $0.042 \pm 0.010$ |
| $SiO_2$ | Si | 20 | $0.063 \pm 0.010$ |
| $SiO_2$ | Si | 40 | $0.045 \pm 0.010$ |
| $MgSiO_3$ | Si | 0 | $0.047 \pm 0.014$ |
| $MgSiO_3$ | Si | 25 | $0.043 \pm 0.008$ |
| $MgSiO_3$ | Si | 50 | $0.047 \pm 0.025$ |
| $MgSiO_3$ | Mg | 0 | $0.135 \pm 0.008$ |
| $MgSiO_3$ | Mg | 25 | $0.092 \pm 0.006$ |
| $MgSiO_3$ | Mg | 50 | $0.084 \pm 0.016$ |

approximately the pressure range studied here, and are associated with an anomalous increase in the diffusivity of the ions that make up the silicate network (Lacks and Van Orman, 2007; de Koker, 2010). Transport of structure-modifying cations (Mg) may also be enhanced by these structural changes, but only in silica-rich compositions (Lacks and Van Orman, 2007). In lower-silica compositions, including $MgSiO_3$, the diffusion of Mg is not as strongly tied to the motions of the silicate network, and its behavior is more like that of an ion in a simple liquid, with diffusive transport becoming less efficient as the density of the liquid increases. The insensitivity of $\beta_{Si}$ to pressure is likely related to the competing effects of densification (which tends to make diffusive motions more cooperative) and changes in melt structure (disruption of the silicate network makes Si diffusion less cooperative). Disruption of the silicate network has a weaker influence on the transport of Mg, and the decrease in $\beta_{Mg}$ with pressure is likely due to a larger number of atoms needing to move cooperatively to allow Mg to diffuse at higher densities.

Our results suggest that further insight on transport processes in silicate melts could be gained by studying the

influence of melt composition and pressure on the isotope effect for different ions. Structure-modifying cations might generally be expected to have $\beta$ that decreases with pressure, particularly in lower-silica melt compositions where cooperative motions with the silicate network are less important. The value of $\beta$ for Si might also be expected to be larger and more sensitive to pressure in very silica-poor melt compositions where no silicate network exists.

Watkins et al. (2011) showed that in chemical diffusion experiments the mass dependence of diffusion for isotopes of an element is correlated with the effective binary diffusion coefficient (EBDC) of the element relative to that of Si. This correlation was found to hold for different elements diffusing in the same melt, and for the same element diffusing in different melts. The correlation was inferred to arise because both $\beta$ and $D_x/D_{Si}$ are related to the degree of coupling between the species of interest and the solvent (represented by Si) – strong coupling to the silicate network reduces both the diffusivity of the cation and its mass dependence. Our MD results on self-diffusion are in qualitative agreement with the experimental trend for chemical diffusion. In particular, the pressure dependence of $\beta$ for Mg found here in simulations of self-diffusion follows the experimental trend for chemical diffusion (Fig. 3). This similarity suggests that the value of $\beta$ in silicate melts is related to the degree of coupling to the silicate network in both chemical diffusion and self-diffusion. Further experimental work on the mass dependence of isotope self-diffusion is needed to test whether this is indeed the case. Although there is a close similarity between the self-diffusion coefficients and the EBDCs for major elements among many experimental studies (Zhang et al., 2010), the difference between these coefficients can be large, particularly when the concentration gradient for the element of interest is large (Liang et al., 1996a,b).

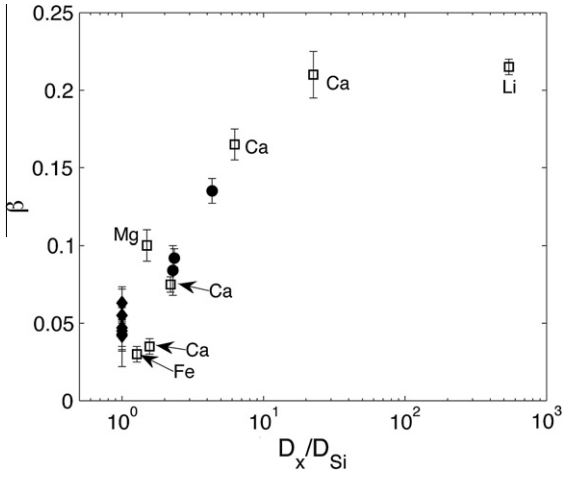


Fig. 3. Correlation between the mass dependence of isotope diffusion ($\beta$) and the diffusivity of the element relative to that of Si (the primary network former). Closed symbols are MD self-diffusion results from this study, at pressures from 1 atm to 50 GPa (circles: Mg; diamonds: Si); open symbols represent experimental effective binary diffusion data for various elements in various silicate melt systems (Richter et al., 2003, 2008, 2009; Watkins et al., 2009, 2011).

Further insight into the cooperative nature of the atomic motions that underlie the isotope effect on diffusion in silicate liquids can be gained by examining how changing the mass of an atom alters the diffusivities of the other atoms in the system. Fig. 4 shows the results of simulations for $SiO_2$ where the fraction of heavy silicon atoms is varied with the mass of the heavy Si atoms being larger by a factor of 10. These results show that the diffusivities of *all* atoms decrease as the fraction of the heavy Si atoms increase, i.e. the diffusivities of the oxygen and normal silicon atoms decrease even though their masses have not changed. This dependence of diffusivities on isotope concentration cannot be described by the commonly used scaling law of Eq. (1), which relates the diffusivity of a species only to the mass of that species. Although natural variations in diffusivity related to changes in the proportions of isotopes of other species are not likely to be significant, the effect is important because it gives insight into the cooperative motions involved in diffusion.

The dependence of the diffusivities of one species on the isotope concentration of other species, and the small dependence of isotope diffusion on mass compared to low-density gases, arise because diffusion in dense fluids is a complex process that involves the cooperative motions of many atoms. As a rule, many atoms must move cooperatively to allow diffusive motions to occur when atoms are tightly packed together in condensed amorphous systems. The cooperative motions involved in diffusion in liquids are often string-like, involving the coupled displacement of a string of many atoms (Donati et al., 1998; Schober, 2002). It should be noted that some small, low-charged species, including neutral He, $CO_2$ and $H_2O$, appear to represent an exception to this rule (Watson, 1994; Zhang and Behrens, 2000; Zhang et al., 2009). These species diffuse relatively rapidly even at temperatures well below the glass transition, where diffusion of silicate network species is

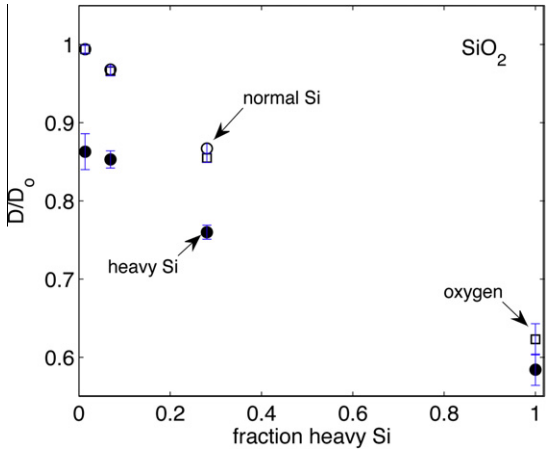


Fig. 4. Changes in diffusivities as the concentration of heavy silicon atoms increases, with the mass of the heavy silicon atoms being 10 times greater than the normal silicon atoms. $D_0$ represents the diffusivity of the element at the same state point ($T$, $P$) with all atoms having normal masses. $T = 4500$ K, $P = 1$ atm. The filled symbols represent the heavy Si atoms, and the open symbols represent normal Si (circles) and normal oxygen (squares).

negligible. This implies that their diffusion is not highly cooperative, but is instead a type of "interstitial" process that involves only small, local elastic motions of the surrounding atoms to allow hops between interstitial sites within the liquid or glass. In these cases where strongly coupled motions are not required for diffusion (as evidenced by significant diffusivity below the glass transition), we would expect the value of $\beta$ to be relatively large. There is some experimental support for this, as He diffuses rapidly in basaltic glasses and also has a relatively large value of $\beta$, ~0.33 at 500 °C (Trull and Kurz, 1999). Similarly, lithium has a relatively large value of $\beta$ and rapid diffusivity in silicate melts (Richter et al., 2003), and also diffuses rapidly in silicate glasses (Jambon and Semet, 1978).

A simple model for the mass dependence of isotope diffusion assumes that a cooperatively diffusing group of atoms follows the same dependence on mass as a molecule within an ideal gas (Kluge and Schober, 2000). According to this simple model the diffusivity ratio of two isotopes scales as

$$\frac{D_2}{D_1} = \left(\frac{m_1^*}{m_2^*}\right)^{1/2} \tag{3}$$

where $m^*$ is the effective mass of the cooperatively diffusing group of atoms and the diffusivity of the isotope is identical to that of the cooperatively diffusing group. This group is considered to consist of $N$ molecular units ($SiO_2$ or $MgSiO_3$) that are moving cooperatively, such that the effective mass is given by

$$M^* = m_{i,j} - \langle m_i \rangle + N\langle m_{mol} \rangle, \tag{4}$$

where $i$ identifies the element and $j$ the isotopic species (light or heavy); $<m_i>$ represents the average atomic mass of the element and $<m_{mol}>$ the average molecular mass of the system, which depend on the isotopic composition. If this simple model were correct, it could be used to find the number of molecular units involved in the cooperative diffusion of each type of atom.

The model can be tested in terms of its prediction of the changes in diffusivity of one species due to changes in the isotopic composition of one or more other species. When the isotopic composition of element $i$ is held constant and only the isotopes of other elements are allowed to vary, $m_{i,j} = \langle m_i \rangle$, and the effective mass of the cooperatively diffusing unit is $m^* = N\langle m_{mol} \rangle$. The diffusivity ratio of an element $i$ in two systems that are identical except in the isotopic composition of elements other than $i$ is then predicted to scale as:

$$\frac{D_{i,2}}{D_{i,1}} = \left(\frac{\langle m_{mol} \rangle_1}{\langle m_{mol} \rangle_2}\right)^{1/2} \tag{5}$$

The predictions of this model are compared with the simulation results in Fig. 5. While the model qualitatively shows the decrease in diffusivity of a species as the mass of one or more other species is increased, the magnitude of the decrease predicted by the model is significantly larger than found in the simulations. Instead of an exponent of ½ in Eq. (4), the data for both $SiO_2$ and $MgSiO_3$ (at all pressures) are consistent with an exponent of ~1/5. Similarly, in liquid MgO the variation in oxygen diffusivity with changes in the average mass of magnesium, from the results of Tsuchiyama et al. (1994), is consistent with an exponent of ~0.12 (with large scatter). Hence, the simple model described above does not fully capture the relationship between cooperative atomic motions and the isotope effect, in liquids consisting of more than one type of atom, and cannot be used to find the number of cooperatively diffusing atoms or molecular units involved in diffusion.

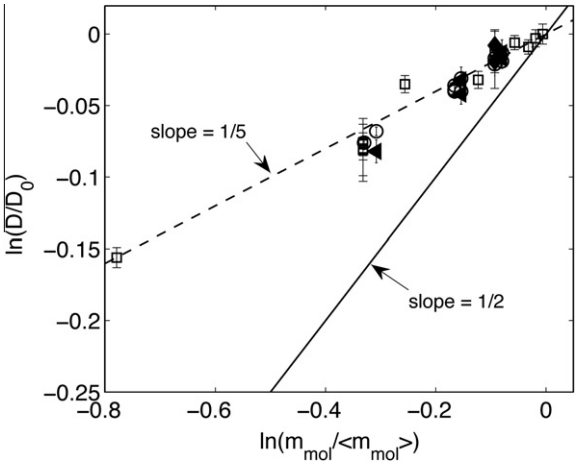


Fig. 5. Variation in diffusivity with changes in the isotopic composition of other species. Squares, oxygen in $SiO_2$, where only the isotopic composition of silicon is changing; circles, oxygen in $MgSiO_3$, where the isotopic composition of magnesium and/or silicon is changing; diamonds, magnesium in $MgSiO_3$ with isotopic composition of silicon changing; triangles, silicon in $MgSiO_3$ with isotopic composition of magnesium changing. Included on the figure are simulation results from all pressures (1 atm to 50 GPa). The simple model described in the text predicts that the data will fall on a line with slope = ½, but the data are instead consistent with a slope of approximately 1/5.

We note that when the atomic mass of every atom in the system is changed uniformly, i.e. is multiplied by the same numerical factor $\lambda$, the diffusivities in the normal system and the system with uniformly altered masses scale as

$$\frac{D_{i,\lambda}}{D_{i,0}} = \left(\frac{m_{mol}}{\lambda m_{mol}}\right)^{1/2} = \lambda^{-1/2} \tag{6}$$

This relationship holds for any system of interacting particles in which quantum effects are negligible (see Appendix). To address the effect of non-uniform variation of the masses of different elements, simulations were carried out for liquid $SiO_2$ in which the masses of normal silicon and oxygen are changed by different factors, $\lambda_{Si}$ and $\lambda_O$. In presenting the results, $\lambda$ represents the factor by which the total system mass changes from the normal (due to variations in the mass of Si and/or O), and $r = \lambda_O/\lambda_{Si}$. Fig. 6 shows the results for $\left(\frac{D_{i,\lambda}}{D_{i,0}}\right)/\lambda^{-1/2}$ as a function of $r$. As expected, $\left(\frac{D_{i,\lambda}}{D_{i,0}}\right)/\lambda^{-1/2} = 1$ when $r = 1$. However, its value becomes larger as $r$ deviates from 1, for both oxygen and silicon. Changing the mass of silicon, for example, but not oxygen, affects the diffusivities of both elements similarly, but not as much as would be expected based on

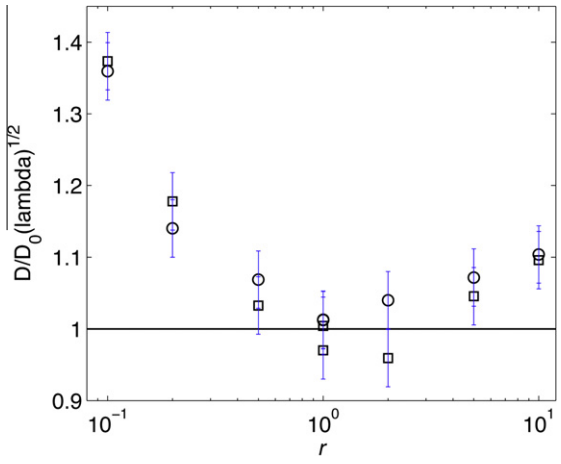


Fig. 6. Results of simulations carried out in which the total mass of the system varies according to the factor $\lambda$, with silicon mass changing by the factor $\lambda_{Si}$, oxygen mass changing by the factor $\lambda_O$, and $r = \lambda_O/\lambda_{Si}$. $D$ is the diffusivity in these simulations, where the masses of Si and/or O are larger than normal, and $D_0$ is the diffusivity in the case of normal masses for all atoms. Circles represent results for silicon, and squares represent results for oxygen. Note that an exact analytic result is $\left(\frac{D_{i,\lambda}}{D_{i,0}}\right)/\lambda^{-1/2}=1$ when $r = 1$, and that there are two sets of data at $r = 1$, corresponding to $\lambda = 2$ and $\lambda = 10$.

uniform mass scaling. The dependence of the diffusivities on the ratio $r$ is likely due to momentum transfer considerations during collisions (Kiriuscheva and Kuzmin, 2005).

## 4. DIFFUSIVE ISOTOPE FRACTIONATION DURING MAGMATIC PROCESSES

Significant fractionation of silicon isotopes by chemical diffusion in igneous systems has generally been considered to be unlikely based on (1) the lack of a measurable isotope effect for Ge in $GeO_2$ (Richter et al., 1999) and (2) the limited variation in $SiO_2$ concentration among natural silicate liquids (less than a factor of ~2). It is worthwhile to re-examine the potential magnitude of diffusive silicon isotope fractionation during magmatic processes based on the significant isotope effect simulated here, and on the increasing ability to measure small variations in isotopic compositions in magmatic samples (presently on the order of ~0.1‰ or less; e.g. Savage et al., 2011).

### 4.1. Diffusive fractionation during crystallization

Crystal growth in magmas can fractionate isotopes via diffusion in the liquid adjacent to the moving crystal interface (Watson and Müller, 2009). Crystallization of olivine in particular has the potential to fractionate Si and Mg isotopes. Olivine is depleted in silica relative to any natural magma, and olivine crystallization therefore leads to a buildup of $SiO_2$ in the liquid that must diffuse away from the crystal surface. Heavy silicon isotopes diffuse more slowly and may therefore become enriched near the crystal surface, if diffusion is slow compared to the rate of crystal growth. If crystal growth is rapid enough, the heavy Si isotope signature that is produced in the near-field liquid can become trapped in the crystal. Magnesium is compatible in olivine and MgO is therefore depleted in the adjacent liquid during growth. Diffusion of MgO is therefore directed toward the olivine surface, and may lead to enrichment of light Mg isotopes in the olivine.

An approximate solution for the steady state isotope composition of a crystal growing in an infinite medium, when the diffusive boundary layer is thin compared to the crystal radius and there is no equilibrium fractionation of isotopes, is (Watson and Müller, 2009):

$$\delta = 1000\left(1 - \frac{D_h}{D_l}\right)\left(\frac{vL}{D_h}\right)(1 - K) \quad (7)$$

where $\delta$ is the difference between the isotope ratio in the crystal and that in the bulk liquid (in ‰), $v$ is the linear crystal growth rate (m/s), $L$ is the boundary layer thickness (m) and $K$ is the equilibrium crystal/liquid element partition coefficient. Fig. 7 shows calculated $\delta^{30}$Si and $\delta^{26}$Mg for an olivine phenocryst as a function of the growth rate $v$. It is possible to fractionate Si and Mg isotopes measurably by diffusion through the boundary layer, but only when the crystal growth rate is quite large, on the order of cm/yr. Diffusive fractionation during olivine crystallization would be expected to generate a negative correlation between $\delta^{30}$Si and $\delta^{26}$Mg, with $\delta^{30}$Si larger in olivine phenocrysts than in the residual liquid. During progressive olivine fractionation, more differentiated magmas would acquire a light Si isotope and heavy Mg isotope signature. Lavas analyzed by Savage et al. (2011) show the opposite sense of fractionation in Si isotopes, with more differentiated lavas having heavier Si isotopes, and hence cannot be explained by diffusive fractionation during fractional crystallization.

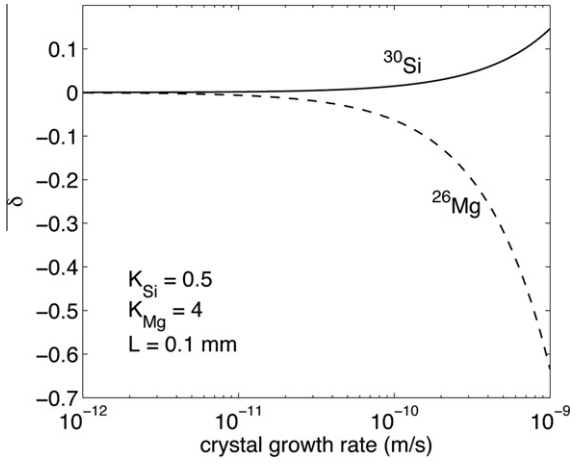


Fig. 7. Calculated (Eq. (7)) steady-state $\delta^{30}$Si and $\delta^{26}$Mg in an olivine phenocryst as a function of its growth rate, where isotope fractionation is due only to diffusion in a diffusive boundary layer adjacent to the growing crystal. The diffusion coefficients assumed for normal Si and Mg are 1.3 and $5.1 \times 10^{-12}$ m$^2$/s, respectively, appropriate for a basaltic liquid at 1100 °C (Zhang et al., 2010). The diffusivity ratios $D^{30}Si/D^{28}Si = 0.9962$ and $D^{26}Mg/D^{24}Mg = 0.9892$ are based on the mass dependences for Si and Mg isotopes determined in this study. The boundary layer adjacent to the phenocryst is assumed to be 100 μm thick, and the crystal/melt partition coefficients for Si and Mg are assumed to be 0.5 and 4, respectively.

However, our results suggest that significant diffusive fractionation of Si isotopes may be found in phenocrysts with textural evidence of rapid growth, and in these cases could provide a sensitive measure of the growth rate.

For Mg, it is important to point out that while diffusion through the liquid boundary layer of a rapidly grown olivine crystal would be expected to impart a light Mg isotope signature to the olivine, the isotopic composition can also be influenced by diffusive fractionation within the olivine. Clear evidence for Fe and Mg isotope fractionation due to diffusion through olivine was found by Teng et al. (2011) in olivine phenocrysts from the Kilauea Iki lava lake in Hawaii. In that case diffusion of Mg out of olivine and into the melt increased its $\delta^{26}$Mg, but fractionation would be in the opposite sense if Mg diffusion were in the opposite direction.

### 4.2. Diffusive fractionation during magma mixing

Isotopes can also be fractionated by interdiffusion between melts of different composition. In cases where uphill diffusion is unimportant, heavy isotopes will become concentrated in the liquid with higher elemental concentration, and light isotopes will become concentrated in the liquid with lower elemental concentration. Within the diffusive boundary layer between rhyolite and basalt, Si will thus become isotopically heavy in the high-$SiO_2$ region, and isotopically light in the low-$SiO_2$ region. On the other hand, elements that are enriched in basalt, like Mg and Fe, will become isotopically light in the high-$SiO_2$ region and isotopically heavy in the low-$SiO_2$ region. The magnitude of isotope fractionation within the boundary layer depends on the ratio of diffusivites of the isotopes, and on the ratio of elemental concentrations in the two liquids. A plot showing countours of the maximum isotope fractionation, calculated as a function of the diffusivity ratio and elemental ratio, is shown in Fig. 8 (after Richter et al., 2003). For Si, our simulation results indicate that resolvable isotope fractionation, up to ~0.5‰, can accompany interdiffusion between basaltic and rhyolitic liquids. For Mg the isotope fractionation can be much greater, up to ~20‰ at atmospheric pressure, due both to the larger contrast in Mg concentration between rhyolitic and basaltic lavas and the larger contrast in diffusivity of Mg isotopes.

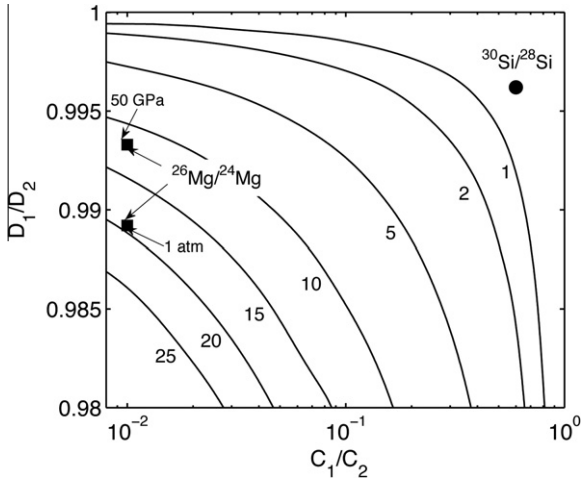


Fig. 8. Contour plot of maximum isotope fractionation resulting from interdiffusion between melts, as a function of the ratio of element concentration in the two liquids and the diffusivity ratio of the isotopes [after Richter et al., 2003]. The numbers on the contour curves indicate the value of $\delta$ in ‰. Also shown are the expected values for $^{30}Si/^{28}Si$ and $^{26}Mg/^{24}Mg$ based on our simulation results and on typical elemental concentration ratios for rhyolite and basalt.

## ACKNOWLEDGMENTS

This work was supported by NSF grants EAR0635819, EAR0944238 and EAR1019749, and by the Ohio Supercomputer Center.

## APPENDIX A

For a system of atoms in which the interactions are governed by classical mechanics, the only way mass affects the trajectory of the atoms is through the equation that determines the acceleration of an atom due to the force on the atom, which is expressed in one dimension as:

$$F_{i,x} = m_i \frac{d^2 x_i}{dt^2}$$

If the masses of all atoms are scaled by a constant factor $\lambda$,

$$m_i' = \lambda m_i$$

this is equivalent to scaling the time by the inverse square root of the same factor:

$$F_{i,x}' = m_i' \frac{d^2 x_i}{dt^2} = \lambda m_i = \frac{d^2 x_i}{dt^2} = m_i \frac{d^2 x_i}{d(t/\lambda^{1/2})^2} = m_i \frac{d^2 x_i}{dt'^2}$$

where

$$t' = t/\lambda^{1/2}$$

That is, if everything gets heavier by the factor $\lambda$, the only difference in the dynamics is that everything moves slower by the factor $\lambda^{1/2}$.

The diffusivity is obtained from the Einstein equation,

$$D = \frac{\langle (\Delta r)^2 \rangle}{\Delta t}$$

where $\Delta r$ is the radial distance an atom has moved from its original position.

If all masses are scaled by $\lambda$, as shown above this is equivalent to scaling time by $\lambda^{-1/2}$, and so the diffusivity scales as $\lambda^{-1/2}$:

$$D' = \frac{\langle (\Delta r)^2 \rangle}{\Delta t'} = \frac{1}{\lambda^{1/2}} \frac{\langle (\Delta r)^2 \rangle}{\Delta t}$$

## REFERENCES

Bourg I., Richter F., Christensen J. and Sposito G. (2010) Isotopic mass dependence of metal cation diffusion coefficients in liquid water. *Geochim. Cosmochim. Acta* **74**, 2249–2256.

de Koker N. P. (2010) Structure, thermodynamics and diffusion in $CaAl_2Si_2O_8$ from first-principles molecular dynamics. *Geochim. Cosmochim. Acta* **74**, 5657–5671.

de Koker N. P., Stixrude S. and Karki B. B. (2008) Thermodynamics, structure, dynamics, and freezing of $Mg_2SiO_4$ liquid at high pressure. *Geochim. Cosmochim. Acta* **72**, 1427–1441.

Donati C., Douglas J. F., Kob W., Plimpton S. J., Poole P. H. and Glotzer S. C. (1998) Stringlike cooperative motion in a supercooled liquid. *Phys. Rev. Lett.* **80**, 2338–2341.

Giordano D. and Dingwell D. B. (2003) Non-Arrhenian multicomponent melt viscosity: a model. *Earth Planet. Sci. Lett.* **208**, 337–349.

Hess B., Kutzner C., van der Spoel D. and Lindhal E. (2008) GROMACS 4: algorithms for highly efficient, load-balanced, and scalable molecular simulation. *J. Chem. Theory Comput.* **4**, 435–447.

Huang F., Chakraborty P., Lundstrom C. C., Holmden C., Glessner J. J. G., Kieffer S. and Lesher C. E. (2010) Composition and temperature independent isotopic fractionation in silicate melts by thermal diffusion. *Nature* **464**, 396–400.

Jambon A. and Semet M. P. (1978) Lithium diffusion in silicate glasses of albite, orthoclase, and obsidian compositions: an ion-microprobe determination. *Earth Planet. Sci. Lett.* **37**, 445–450.

Kiriuscheva N. and Kuzmin S. V. (2005) Influence of mass difference on dynamic properties of isotope mixtures. *Physica A* **352**, 509–521.

Kluge M. and Schober H. R. (2000) Isotope effect of diffusion in a simple liquid. *Phys. Rev. E* **62**, 597–600.

Kyser T. K., Lesher C. E. and Walker D. (1998) The effects of liquid immiscibility and thermal diffusion on oxygen isotopes in silicate liquids. *Contrib. Mineral. Petrol.* **133**, 373–381.

Lacks D. J. and Van Orman J. A. (2007) Molecular dynamics investigations of viscosity, chemical diffusivities and partial molar volumes of liquids along the $MgO–SiO_2$ join as functions of pressure. *Geochim. Cosmochim. Acta* **71**, 1312–1323.

Lacks D. J., Goel G., Bopp C. J., Van Orman J. A., Lesher C. E. and Lundstrom C. C. (2012) Isotope fractionation by thermal diffusion in silicate melts. *Phys. Rev. Lett.* **108**, 065901.

Liang Y., Richter F. M., Davis A. M. and Watson E. B. (1996a) Diffusion in silicate melts, I: self-diffusion in $CaO–Al_2O_3–SiO_2$ at 1500 °C and 1 GPa. *Geochim. Cosmochim. Acta* **60**, 4353–4367.

Liang Y., Richter F. M. and Watson E. B. (1996b) Diffusion in silicate melts, II: multicomponent diffusion in $CaO–Al_2O_3–SiO_2$ at 1500 °C and 1 GPa. *Geochim. Cosmochim. Acta* **60**, 5021–5035.

Lundstrom C. C. (2009) Hypothesis for the origin of convergent margin granitoids and Earth's continental crust by thermal migration zone refining. *Geochim. Cosmochim. Acta* **73**, 5709–5729.

Plimpton S. (1995) Fast parallel algorithms for short-range molecular dynamics. *J Comp Phys*, **117**, 1–19. http://lammps.sandia.gov.

Richter F. M., Liang Y. and Davis A. M. (1999) Isotope fractionation by diffusion in molten oxides. *Geochim. Cosmochim. Acta* **63**, 2853–2861.

Richter F. M., Davis A. M., DePaolo D. J. and Watson E. B. (2003) Isotope fractionation by chemical diffusion between molten basalt and rhyolite. *Geochim. Cosmochim. Acta* **67**, 3905–3923.

Richter F. M., Watson E. B., Mendybaev R., Teng F.-Z. and Janney P. (2008) Magnesium isotope fractionation in silicate melts by chemical and thermal diffusion. *Geochim. Cosmochim. Acta* **27**, 206–220.

Richter F. M., Watson E. B., Mendybaev R., Dauphas N., Georg B., Watkins J. and Valley J. (2009) Isotopic fractionation of the major elements of molten basalt by chemical and thermal diffusion. *Geochim. Cosmochim. Acta* **73**, 4250–4263.

Saika-Voivod I., Sciortino F. and Poole P. H. (2001) Computer simulation of liquid silica: Equation of state and liquid–liquid phase transition. *Phys. Rev. E* **63**, 011202.

Savage P. S., Georg R. B., Williams H. M., Burton K. W. and Halliday A. N. (2011) Silicon isotope fractionation during magmatic differentiation. *Geochim. Cosomochim. Acta* **75**, 6124–6139.

Schober H. R. (2001) Isotope effect in the diffusion of binary liquids. *Solid State Commun.* **119**, 73–77.

Schober H. R. (2002) Collectivity of motion in undercooled liquids and amorphous solids. *J. Non-Cryst. Solids* **307–310**, 40–49.

Teng F.-Z., Dauphas N., Helz R. T., Gao S. and Huang S. (2011) Diffusion-driven magnesium and iron isotope fractionation in Hawaiian olivine. *Earth Planet. Sci. Lett.* **308**, 317–324.

Trull T. W. and Kurz M. D. (1999) Isotopic fractionation accompanying helium diffusion in basaltic glass. *J. Mol. Struct.* **485–486**, 555–567.

Tsuchiyama A., Kawamura K., Nakao T. and Uyeda C. (1994) Isotopic effects on diffusion in MgO melt simulated by the molecular dynamics (MD) method and implications for isotopic mass fractionation in magmatic systems. *Geochim. Cosmochim. Acta* **58**, 3013–3021.

van Beest B. W. H., Kramer G. J. and van Santen R. A. (1990) Force fields for silicas and aluminophosphates based on *ab initio* calculations. *Phys. Rev. Lett.* **64**, 1955–1958.

Vollmayr K., Kob W. and Binder K. (1996) Cooling-rate effects in amorphous silica: A computer-simulation study. *Phys. Rev. B* **54**, 15808–15827.

Watkins J., DePaolo D. J., Huber C. and Ryerson F. (2009) Liquid composition-dependence of calcium isotope fractionation during diffusion in molten silicates. *Geochim. Cosmochim. Acta* **73**, 7341–7359.

Watkins J. M., DePaolo D. J., Ryerson F. J. and Peterson B. T. (2011) Influence of liquid structure on diffusive isotope separation in molten silicates and aqueous solutions. *Geochim. Cosmochim. Acta* **75**, 3103–3118.

Watson E. B. (1994) Diffusion in volatile-bearing magmas. *Rev. Mineral.* **30**, 371–411.

Watson E. B. and Baxter E. F. (2007) Diffusion in solid-Earth systems. *Earth Planet. Sci. Lett.* **253**, 307–327.

Watson E. B. and Müller T. (2009) Non-equilibrium isotopic and elemental fractionation during diffusion-controlled crystal growth under static and dynamic conditions. *Chem. Geol.* **267**, 111–124.

Zhang Y. and Behrens H. (2000) $H_2O$ diffusion in rhyolitic melts and glasses. *Chem. Geol.* **169**, 243–262.

Zhang L., Van Orman J. A. and Lacks D. J. (2009) The influence of atomic size and charge of dissolved species on the diffusivity and viscosity of silicate melts. *Am. Mineral.* **94**, 1735–1738.

Zhang Y., Ni H. and Chen Y. (2010) Diffusion data in silicate melts. *Rev. Mineral. Geochem.* **72**, 311–408.

*Associate editor:* Fred Moynier